

Drift chamber resolution with field off

Maher Quraan

October 14, 2004

This note is a continuation of the previous work and is aimed at understanding issues related to the resolution including effects of multiple scattering, electronic smearing, time offset, STR corrections, and plane alignments. Comparisons with the Monte Carlo and Garfield are included.

Few other modifications were also made in the calculation of the resolution including rejecting tracks with a small angle ($1.5 \text{ deg} < \theta < 5.0 \text{ deg}$), installing the resolution as a function from a fit to the data (rather than using discrete resolution bins), and adjusting the plane position corrections. Figure 1 shows the resolution as a function of drift distance after these modifications are made. A slight improvement at the few micron level is seen as well as a smoother distribution. The black curve is a polynomial fit to the data and is used to weight the hits. Figures 2 and 3 show the tracking residuals binned in distance from the wire. As before, each bin is $100\mu\text{m}$ wide, with the first bin centered at $50\mu\text{m}$.

Figure 4 is the same as figure 1 with various other calculations superimposed. The red dots are the drift chamber resolution calculated from data. The blue dots are calculated from the Monte Carlo with a 1.5ns constant time smearing and a $140\mu\text{m}$ cluster separation. The Monte Carlo calculation used $75\text{MeV}/c$ positrons which were found to undergo the same amount of multiple scattering as $120\text{MeV}/c$ pions (see below). The blue line shows the level of track smearing as a result of multiple scattering for $75\text{MeV}/c$ positrons ($120\text{MeV}/c$ pions). This imposes a lowest possible limit on the resolution for such a beam, constant across the cell. Electronic time jitter provides another contribution to the resolution. Unlike multiple scattering, however, a constant time jitter results in a bigger contribution to the spatial resolution at small distances. The pink curve shows the contribution of a 1.5ns to the resolution. The green curve is a Garfield calculation (provided by Vladimir) with the blue multiple scattering line and the pink electronic smearing curve added to it (in quadrature).

Figures 5 and 6 demonstrate that $120\text{MeV}/c$ pions undergo the same amount of multiple scattering as do $75\text{MeV}/c$ positrons. In both cases a pencil beam was started in plane 7 and directed along the z axis. Figure 5 shows the transverse position of the beam in plane 14. These distributions give a $\sigma \sim 200\mu\text{m}$. Figure 6 shows the scattering angle distribution at plane 14. These distributions have a $\sigma \sim 2.4\text{mrad}$. Despite this relatively large spread in multiple scattering, as demonstrated above, the contribution of multiple

scattering to the chamber resolution is $\sim 20\mu m$.

Figure 7 shows the χ^2 distribution (per degree of freedom) for the Monte Carlo without (top left) and with (top right) multiple scattering turned on, as well as the tracking residuals distributions for the same cases. Figure 8 shows the corresponding distributions for the data on the left, with the MC distributions re-plotted on the same page for comparisons (note, however, that the comparison of the mean and rms is a bit misleading since the MC had a χ^2 cut at 20 while the data had no χ^2 cut).

Figure 9 shows the track-intercept distributions (top) at the origin (plane 7). As may be inferred from the figure, the beam in this run was steered off centre. This is also evident in the ϕ and θ distributions (bottom), where the latter is only plotted for tracks used in the resolution calculation (i.e. after cuts are imposed). Figure 10 shows the same for the Monte carlo.

Figure 11 shows the means of the tracking residuals for the eight planes used in the fit. The red triangles are the means calculated with the standard plane position corrections as provided by CFM. These are then used to further correct the plane positions, and result in the blue dots, all of which are within $\pm 5\mu m$. The green dots are means of the tracking residuals as calculated from the Monte Carlo.

In the previous calculation of the resolution the STRs were iterated, and resulted in a relatively large correction to Garfield particularly at small distance from the wire. As pointed out in that posting, the calculation would also include an overall time offset correction. In order to separate the effect of a constant time offset correction and an STR correction the previous STR correction was removed and the χ^2 and tracking residuals distributions were computed for various time offsets. Figure 12 shows the result of this calculation, with the minimum corresponding to a time offset in the range $3.5 - 4.5ns$. Further investigation of this (by looking at the binned tracking residuals, particularly close to the wire since this is where a time offset has the biggest impact) revealed that a $3.5ns$ gave the best result. An attempt was then made to iterate the Garfield STRs, however, only a small correction was needed as shown in figure 13. The black curve is a fit which is used to correct the time in the tracking.

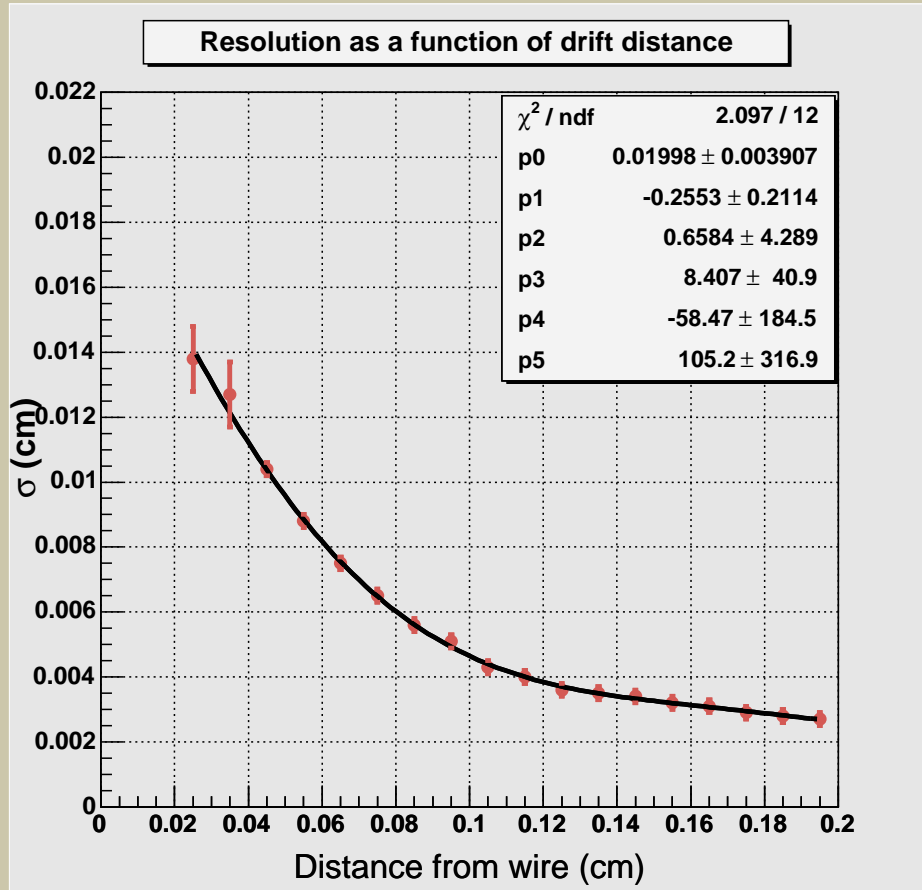


Figure 1: Spatial resolution of the drift chamber as a function of drift distance calculated for 120 MeV/c pions with field off restricted to tracks in the range $1.5^\circ < \theta < 5^\circ$. The curve is a polynomial fit to the data and is used to weight tracks in the Kalman filter.

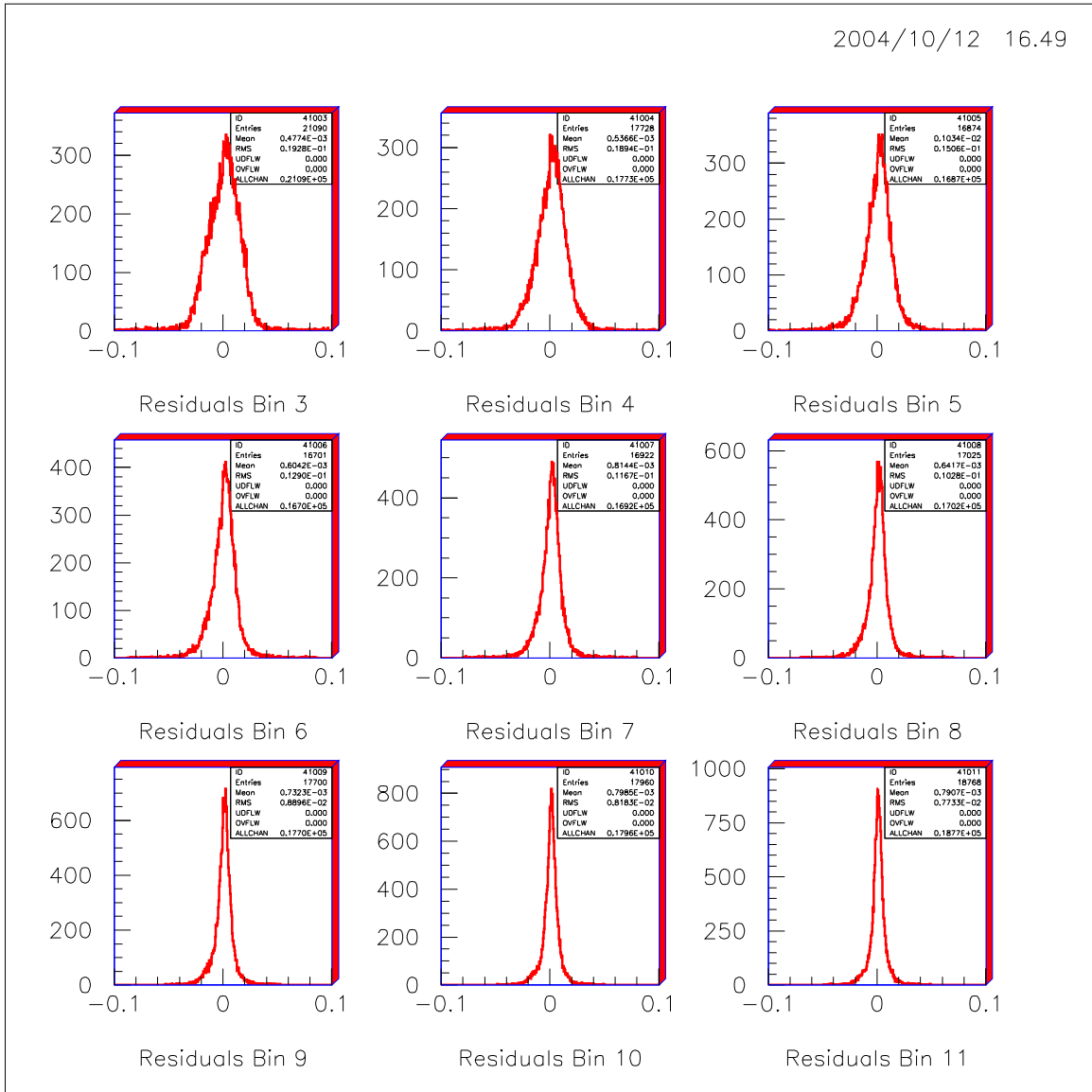


Figure 2: Tracking residual distributions binned in distance from the wire. Each bin is 100 μm wide with the first bin centered at 50 μm (bin 3 corresponds to 250 μm).

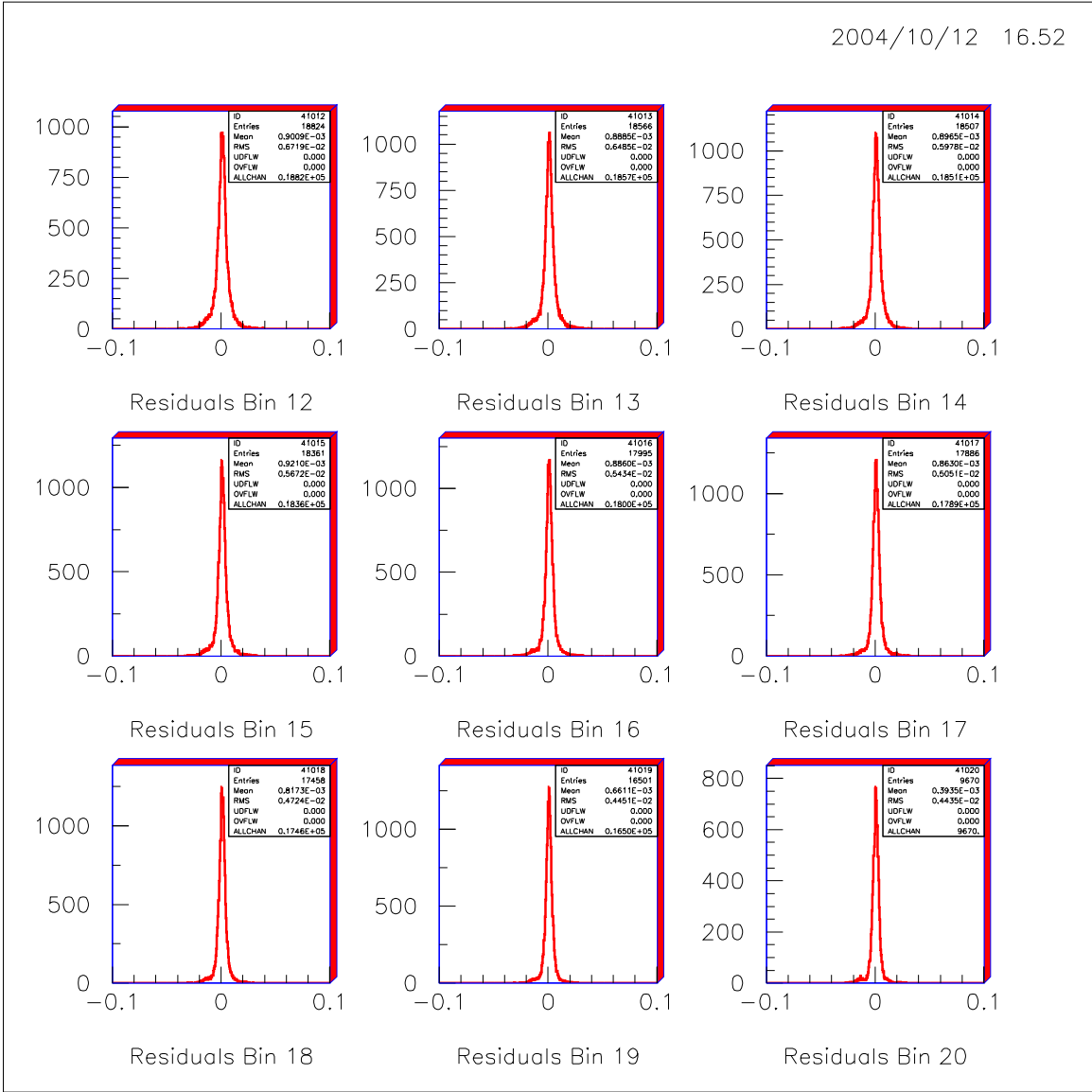


Figure 3: Tracking residual distributions binned in distance from the wire (continued from figure 3).

Chamber resolution as a function of drift distance

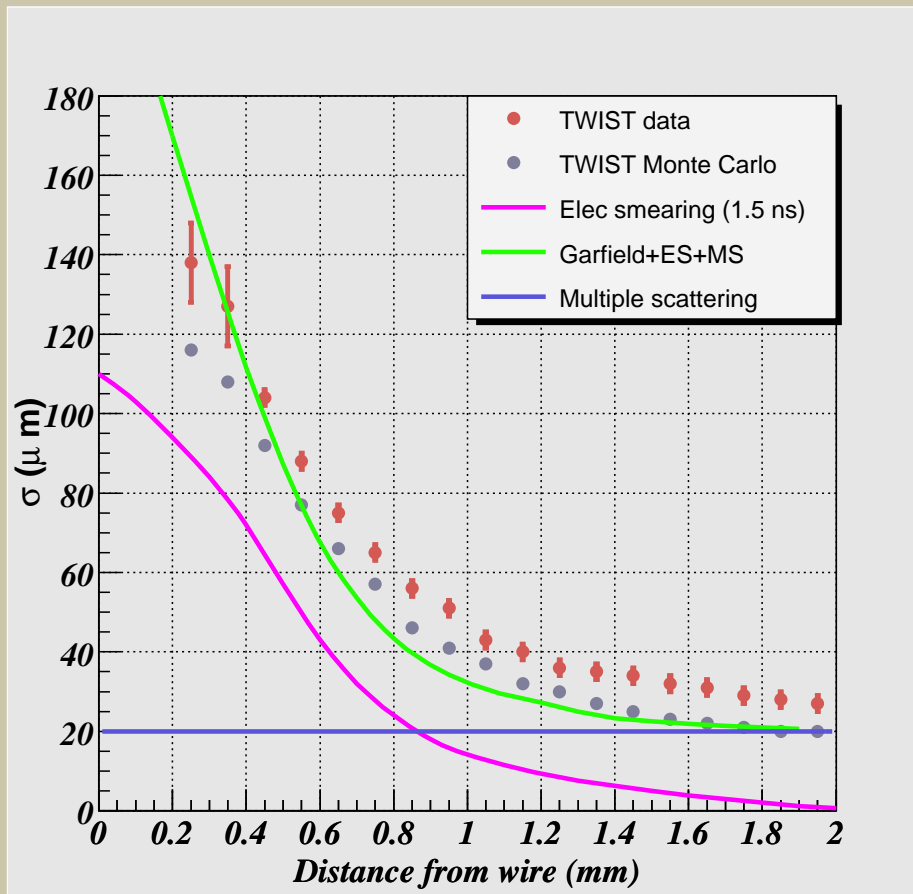
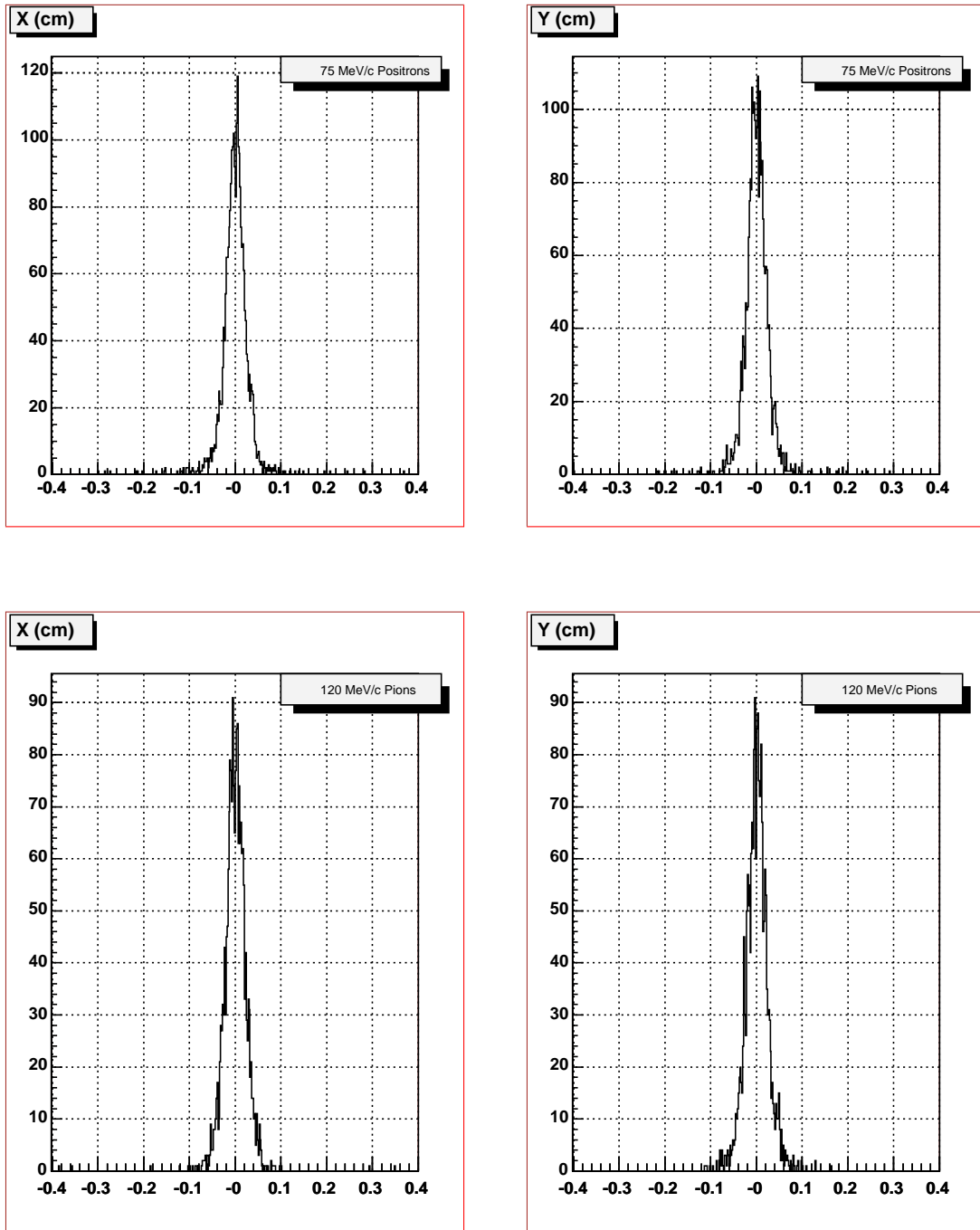


Figure 4: Same as figure 1 with various other calculations added to the figure as listed in the legend (see the text for details).

Multiple scattering



7

Figure 5: Transverse distributions of a 75 MeV/c positron pencil beam (top) and 120 MeV/c pion pencil beam (bottom) started at plane 7 and plotted at plane 14.

Multiple scattering

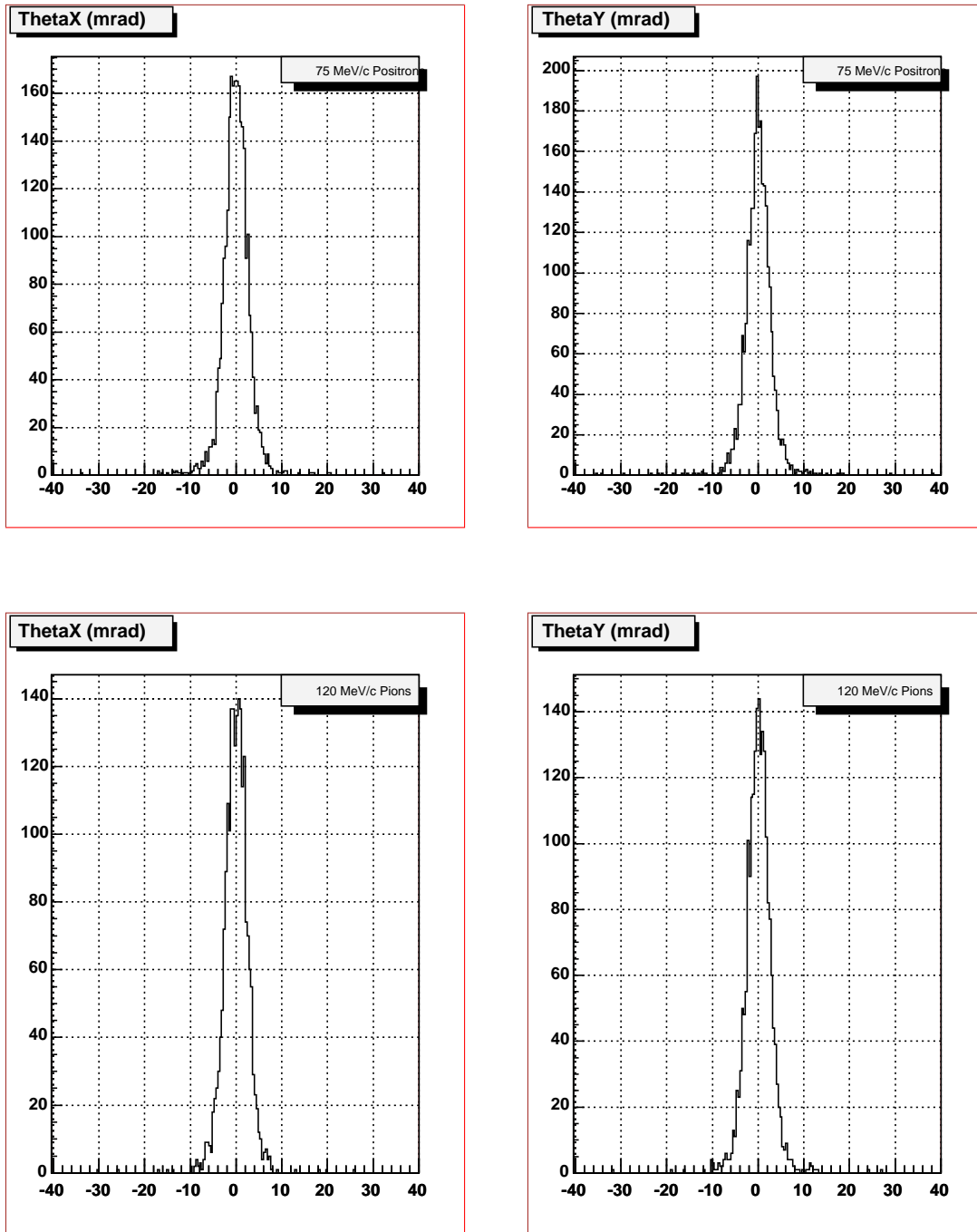
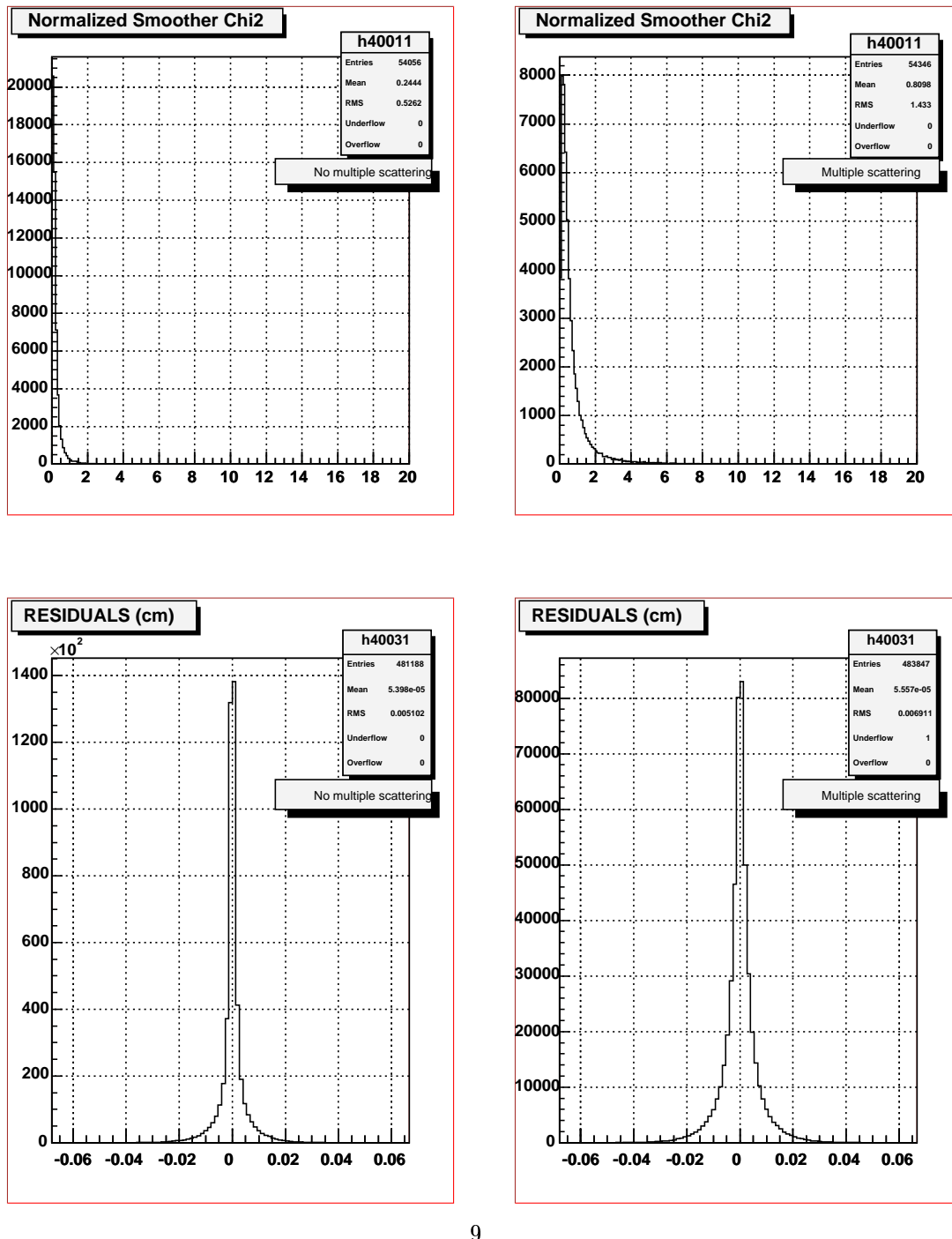


Figure 6: Scattering angles of a 75 MeV/c positron pencil beam (top) and 120 MeV/c pion pencil beam (bottom) started at plane 7 and plotted at plane 14. The beam is directed along the z axis.

Monte Carlo



9

Figure 7: Top left: χ^2 distribution for MC with multiple scattering turned off. Top right: χ^2 for MC with multiple scattering turned on. Bottom left: Tracking residuals for MC with multiple scattering turned off. Bottom right: Tracking residuals distributions with multiple scattering turned on.

Data vs Monte Carlo

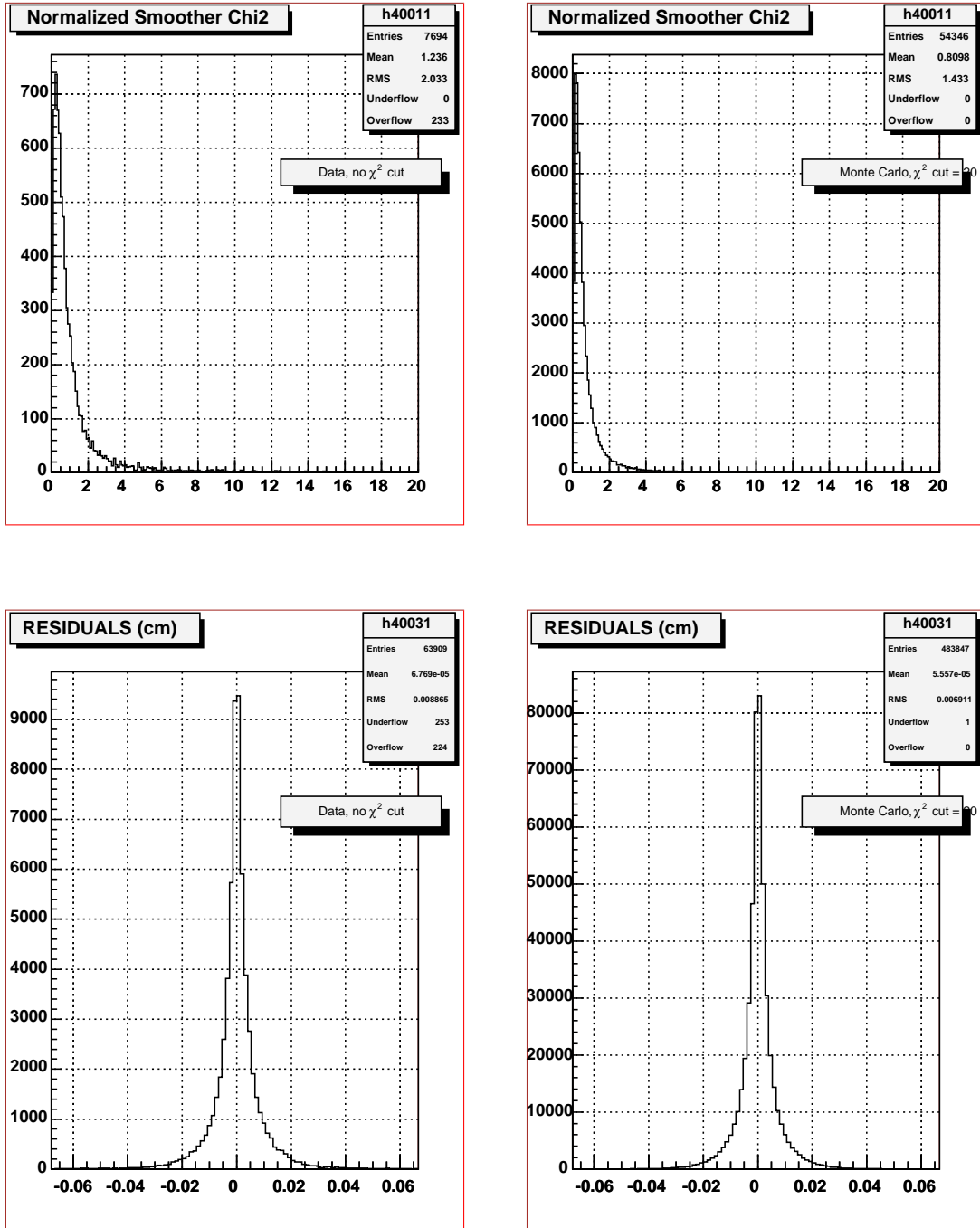


Figure 8: Top left: χ^2 distribution for data. Top right: χ^2 distribution for MC. Bottom left: Tracking residuals distribution for data. Bottom right: Tracking residuals distribution for MC.

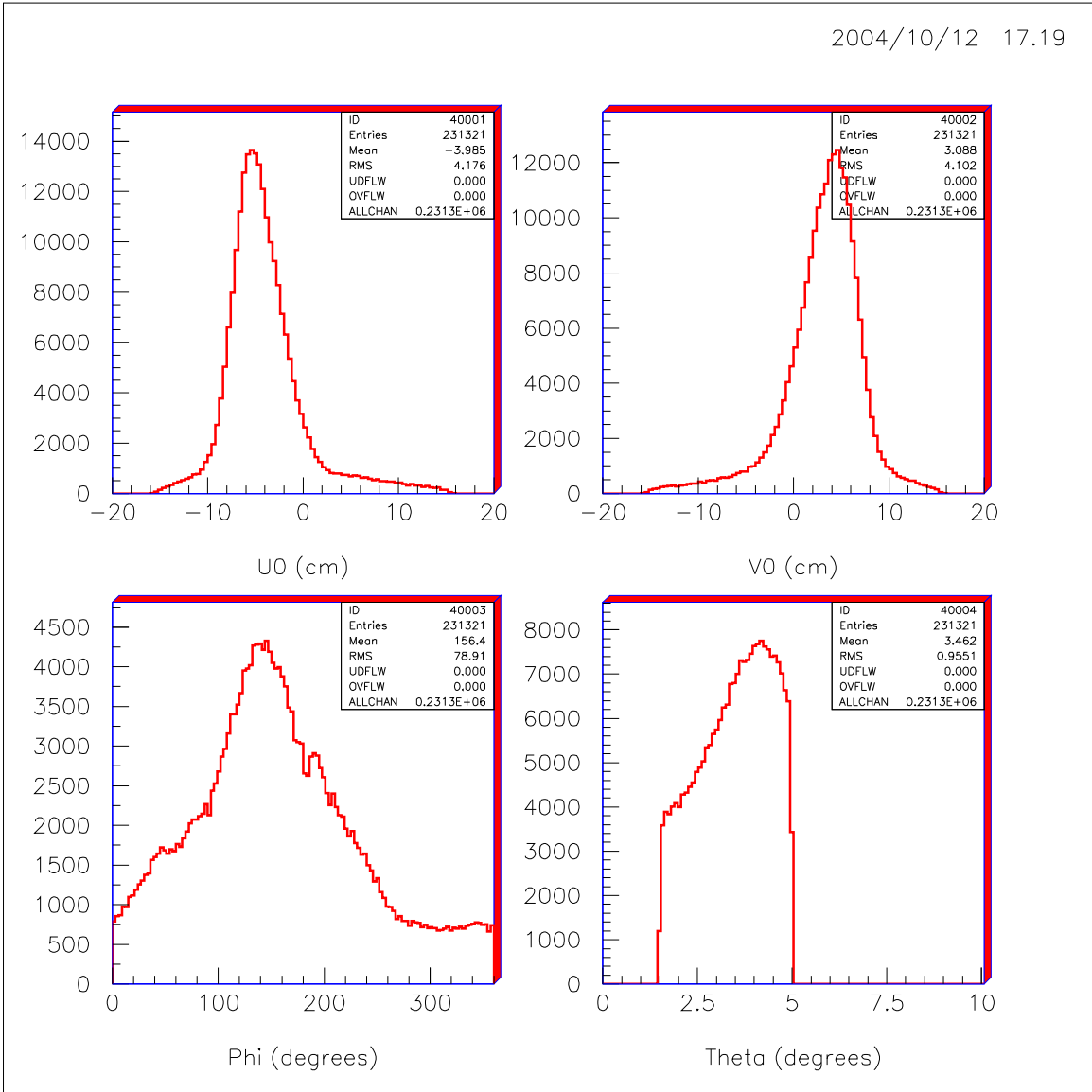


Figure 9: Top: (u,v) position of the track intersection at plane 7 for data. Bottom: Angular distributions of tracks used to calculate the spatial resolution for data.

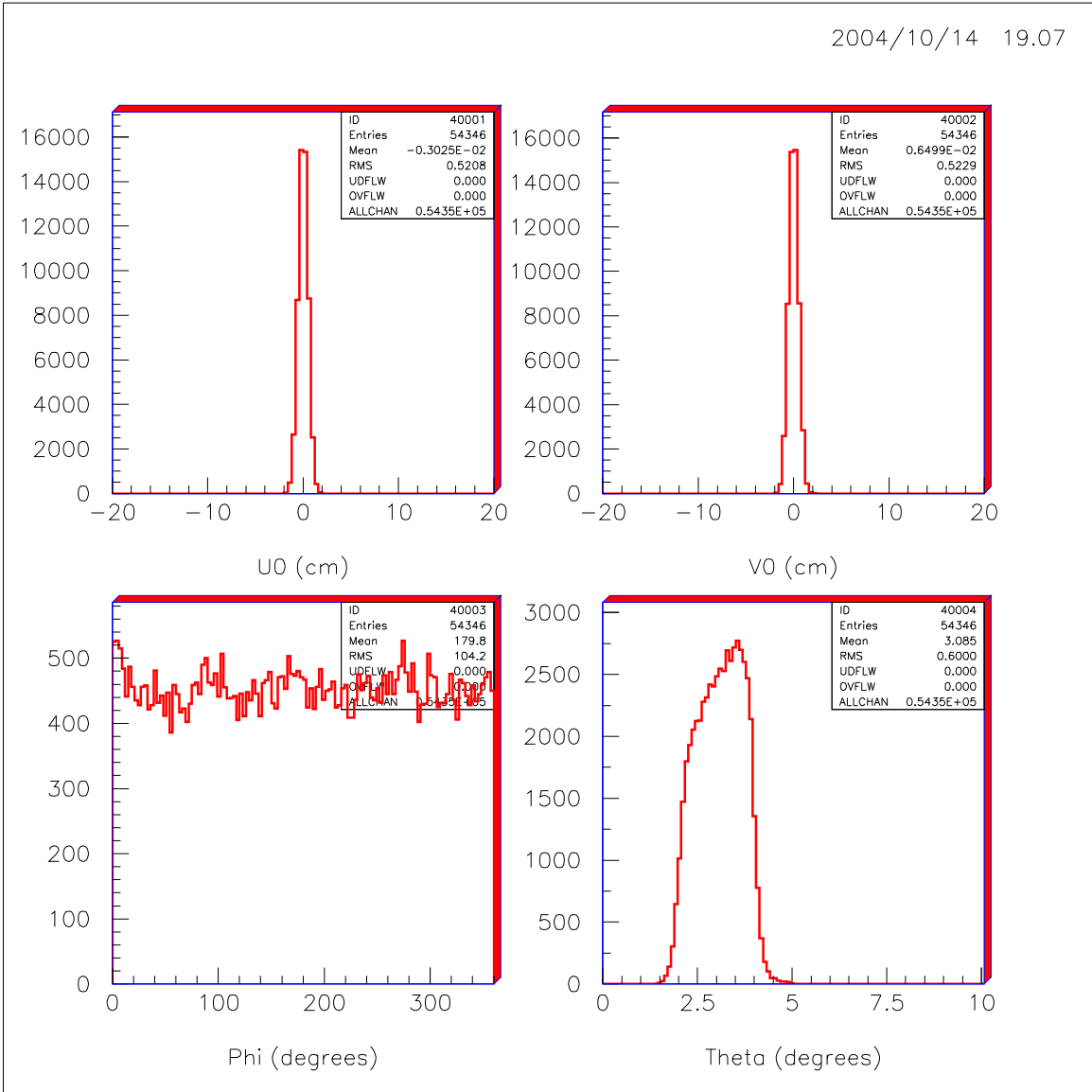


Figure 10: Top: (u,v) position of the track intersection at plane 7 for MC. Bottom: Angular distributions of tracks used to calculate the spatial resolution for MC.

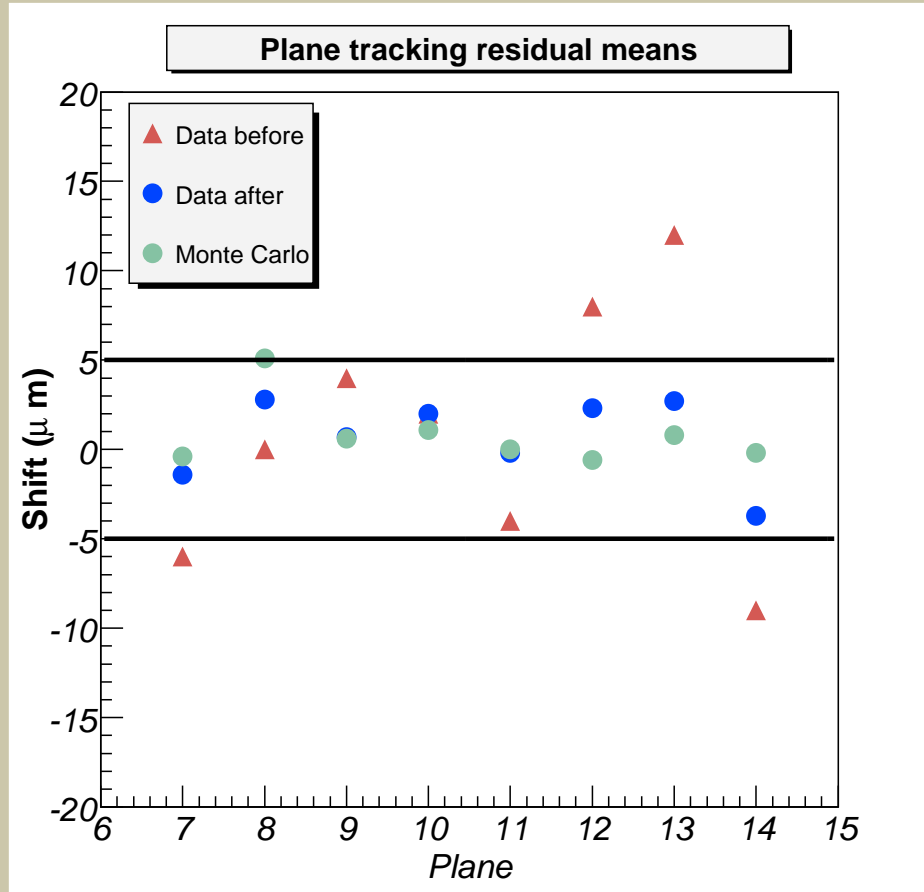


Figure 11: Tracking residual means for the eight planes used in the fit. The red triangles are obtained with the plane rotation corrections as in CFM, the blue dots are after further corrections, and the green dots are for Monte Carlo.

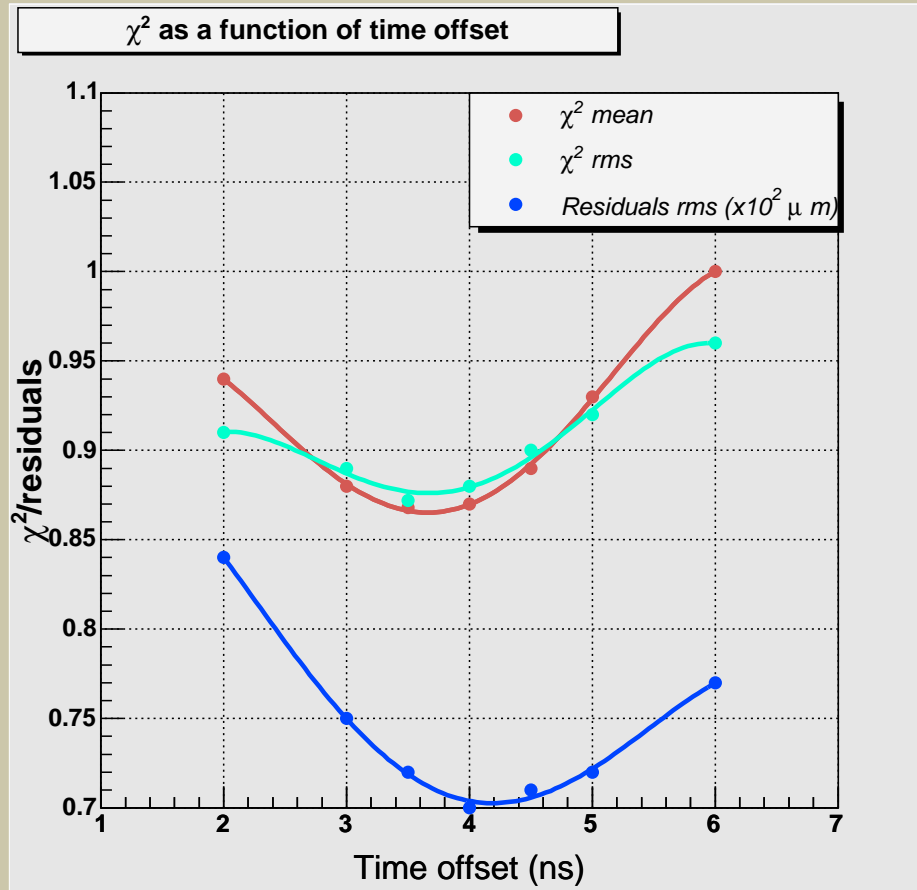


Figure 12: Mean (red dots) and RMS (green dots) of the χ^2 distribution as a function of a global time offset, and RMS of the tracking residuals (blue dots) distribution as a function of the same.

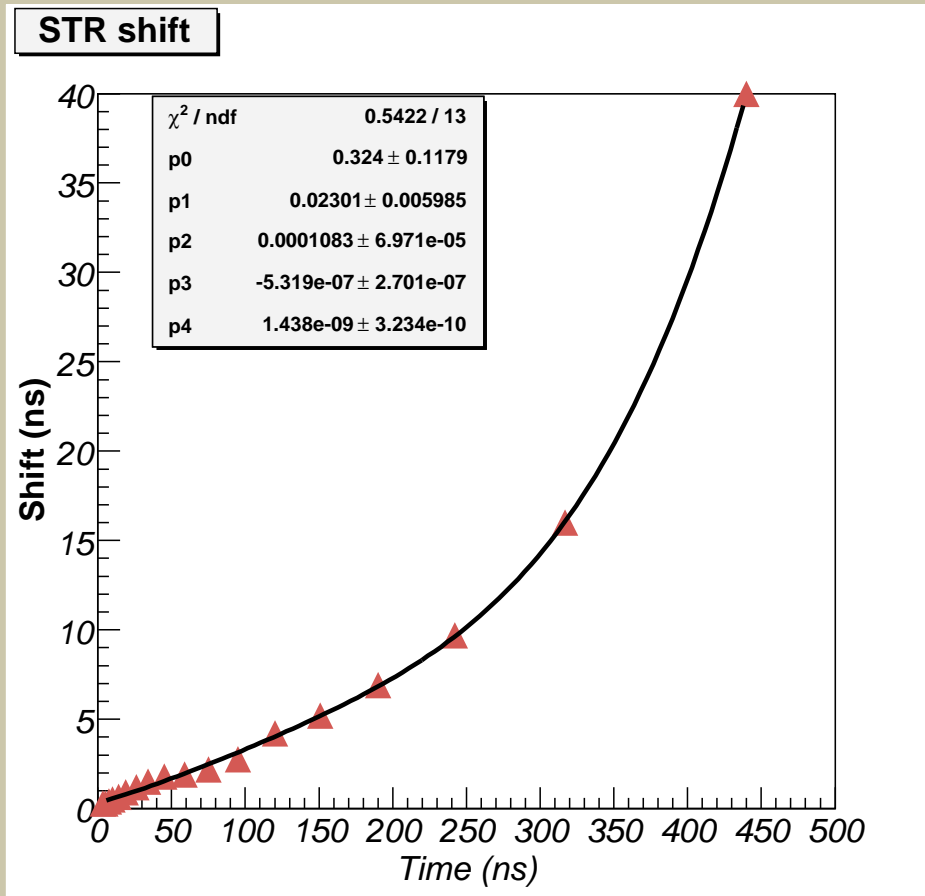


Figure 13: Time correction used to center the means of the tracking residuals after a global 3.5 ns time shift.